

# Towards Generalizable Scene Change Detection

Jae-woo Kim<sup>1</sup> Uehwan Kim<sup>2</sup>,  
**kjw01124@gm.gist.ac.kr, uehwan@gist.ac.kr**

## Abstract

Scene Change Detection (SCD) is vital for applications such as visual surveillance and mobile robotics. However, current SCD methods exhibit a bias to the temporal order of training datasets and limited performance on unseen domains; conventional SCD benchmarks are not able to evaluate generalization or temporal consistency. To tackle these limitations, we introduce a Generalizable Scene Change Detection Framework (GeSCF) in this work. The proposed GeSCF leverages localized semantics of a foundation model without any re-training or fine-tuning—for generalization over unseen domains. Specifically, we design an adaptive thresholding of the similarity distribution derived from facets of the pre-trained foundation model to generate initial pseudo-change mask. We further utilize Segment Anything Model’s (SAM) class-agnostic masks to refine pseudo-masks. Moreover, our proposed framework maintains commutative operations in all settings to ensure complete temporal consistency. Finally, we define new metrics, evaluation dataset, and evaluation protocol for Generalizable Scene Change Detection (GeSCD). Extensive experiments demonstrate that GeSCF excels across diverse and challenging environments—establishing a new benchmark for SCD performance.

## Introduction

Scene Change Detection (SCD) (Radke et al. 2005) is essential in multiple applications including visual surveillance (Wu et al. 2020), anomaly detection (Huang et al. 2022), mobile robotics (Nehmzow et al. 2000), and autonomous vehicles (Janai et al. 2017). SCD involves identifying the changes in the current scene compared to those at different time steps. The SCD task is challenging due to various factors such as illumination variations, seasonal changes, and weather conditions. To cope with these challenges, recent studies in SCD have leveraged deep-learning algorithms to extract discriminative and robust features that can effectively distinguish meaningful changes in a scene.

However, current deep learning-based SCD methods hardly display the reported performance when applied outside the temporal conditions or environments in which they were trained. Concretely, they tend to memorize the temporal sequence of scenes in the training set—leading to inconsistent predictions between  $t_0$  (reference)  $\rightarrow t_1$  (query) and  $t_1$  (reference)  $\rightarrow t_0$  (query). Moreover, their performance

Method	Generalizable Scene Change Detection		
	Seen Domain	Unseen Domain	Temporal Consistency
CS3DNet	✓	✗	✗
CDResNet	✓	✗	✗
DR-TANet	✓	✗	✗
C-3PO	✓	✗	△
<b>GeSCF (Ours)</b>	✓	✓	✓

Table 1: Comparison between existing SCD methods and our proposed GeSCF in terms of GeSCD.

drops sharply when deployed to an environment with different visual features rather than the trained ones. These results indicate that current SCD approaches are susceptible to over-fitting—resulting in exaggerated performance over the benchmark datasets (Table 1 summarizes the limitations of existing SCD methods compared to our GeSCF). Furthermore, current SCD evaluation protocols are not capable of treating the temporal consistency of predictions and unseen domain performance.

To overcome the limitations and develop a method that could readily function regardless of temporal and environmental factors, we propose *Generalizable Scene Change Detection Framework* (GeSCF)—focusing on the temporal consistency and generalizability of SCD algorithms. We rethink the SCD problem from the lens of feature similarity distribution derived from a large-scale pre-trained model, i.e., a foundation model (Mu et al. 2022). Specifically, GeSCF utilizes the localized semantics encoded by a foundation model for each temporal image. We generate initial pseudo-change masks by analyzing and thresholding the similarity distribution of bi-temporal features. Furthermore, we refine pseudo-change masks through comparison with the Segment Anything Model’s (SAM) (Kirillov et al. 2023) class-agnostic masks, enhancing the performance of our scene change detection. Overall, the proposed GeSCF performs zero-shot SCD, free of costly change annotation and sparse training sets which are critical issues in the SCD task.

In addition, we develop new metrics, evaluation dataset, and evaluation protocol—establishing a cornerstone for

**Generalizable Scene Change Detection (GeSCD).** We measure the intersection between two temporal order predictions to evaluate the temporal consistency quantitatively. Further, we propose a new evaluation dataset—the ChangeVPR dataset—to assess the robustness of SCD approaches in various unseen environments, including urban, suburban, and rural settings. Existing real-world SCD datasets, which only contain a few urban scenarios, do not reflect the diversity of the scene images—highlighting the importance of our contribution. Extensive experimental results demonstrate that the proposed GeSCF significantly outperforms prior state-of-the-art methods in detecting changes in unseen domains without any training and performs on-par with the fine-tuned SCD models for specific datasets.

In summary, our contributions are the following:

1. **Problem formulation:** We define *GeSCD* that induces a robust SCD algorithm regardless of temporal order and environmental factors. To the best of our knowledge, this is the first comprehensive effort to address the generalization problem in SCD research with a substantial performance gain in unseen domains.
2. **Model design:** We design a *GeSCF* that utilizes localized semantics of a foundation model and their similarity distribution to generate robust change masks in addition to bi-temporal mask refinement using SAM’s class-agnostic masks.
3. **Benchmark set up:** We propose a set of new metrics, evaluation dataset, and evaluation protocols that effectively measures an SCD model’s generalizability and temporal consistency under comprehensive conditions.
4. **Ablation study:** We design and conduct a set of extensive ablation studies to reveal crucial insights for constructing generalizable SCD models.

## Related Works

**Change Detection:** Change Detection (CD) research largely falls into three categories based on the data characteristic: remote sensing CD, video sequence CD, and indoor/outdoor scene CD (ours). First, remote-sensing CDs handle data collected from satellite or aerial platforms to detect surface changes in area over time. Several works proposed supervised (Saha et al. 2022; Chen et al. 2022; Bernhard, Strauß, and Schubert 2023), semi-supervised (Hao et al. 2023; Bandara and Patel 2022), and unsupervised frameworks (Bergamasco et al. 2022; Noh et al. 2022) in remote sensory scenes to overcome data scarcity. Moreover, video sequence CDs (Mandal et al. 2020; Akilan et al. 2020) focus on segmenting a frame into the foreground and background regions corresponding to object motion. These CD approaches, however, assume perfect alignment between query and reference images—an assumption often fails in real-world settings. In our work, we would focus on indoor/outdoor Scene CD and refer to the task as SCD.

**Scene Change Detection (SCD):** For SCD, CDNet (Sakurada et al. 2017) concatenates bi-temporal images and their estimated optical flow to obtain change masks. CSCD-Net (Sakurada, Shibuya, and Wang 2018) utilizes two correlation layers (Dosovitskiy et al. 2015), then concatenate

each output to feed the decoder. DR-TANet (Chen, Yang, and Stiefelhagen 2021) introduces the attention mechanism and proposes CHVA (Chen, Yang, and Stiefelhagen 2021) to refine the change masks, and C-3PO (Wang, Gao, and Wang 2023) proposes sequential feature mixing of bi-temporal images from temporal to spatial order, feeding the mixed features to off-the-shelf semantic segmentation models. Several works (Park et al. 2022; Lee and Kim 2024) utilize synthetic datasets in combination with flow estimation to train SCD models. However, all these SCD models rely on supervised or semi-supervised methods optimized and evaluated for a specific benchmark dataset without assessing their performance on unseen domains—leading to low generalizability.

The generalizability of SCD algorithms relies on two key factors: temporal consistency and cross-domain performance. Temporal consistency ensures that the binary change detector does not overfit to any specific temporal direction, maintaining undirected algorithms (Zheng et al. 2021). Cross-domain performance ensures robust operation on unseen data, making the model adaptable to arbitrary change scenarios. Although several works proposed a self-supervised pre-training strategy (Ramkumar, Arani, and Zonooz 2022) or temporal symmetry (Wang, Gao, and Wang 2023) for SCD, they still exhibit a significant performance gap in unseen domains. Moreover, the symmetric structure relies on a specific prior knowledge of the domain—rendering it impractical for unknown domains without the proper inductive bias. In contrast, our GeSCF stands as a unified framework, demonstrating robust performance on unseen data while preserving a symmetric structure across all settings.

**Foundation Models:** Foundation models demonstrate strong capabilities across various applications with large-scale training sets and versatile training strategies. For example, DINO (Caron et al. 2021) and its successor, DINOv2 (Oquab et al. 2023), implement joint embedding strategies with losses at the image-level and combined image-/token-levels, respectively. CLIP (Radford et al. 2021) leverages contrastive learning techniques utilizing image and textual data. Moreover, SAM (Kirillov et al. 2023) trained under a fully supervised framework with SA-1B (Kirillov et al. 2023) dataset excels in identifying visual elements and generates detailed semantic masks for unseen images. Considering the close relation between change detection and the segmentation task as corroborated in (Zheng et al. 2021; Ding et al. 2023; Wang, Gao, and Wang 2023; Mei et al. 2024), we employ SAM ViT (Dosovitskiy et al. 2020) to extract visual features for our proposed framework.

Among CD methods, several works leveraged SAM with learnable adaptors (Ding et al. 2023; Mei et al. 2024) and thresholding strategy (Chen and Bruzzone 2022) to enhance performance on remote sensing CD. However, a fundamental difference in our approach is that we use SAM’s internal byproducts and their skewness to binarize the change candidate and utilize its output mask to obtain prior information on bi-temporal scene semantics without any learnable parameters (Yu et al. 2023; Xie et al. 2023; Ahmadi et al. 2023; Giannakis et al. 2023; Chen et al. 2023).

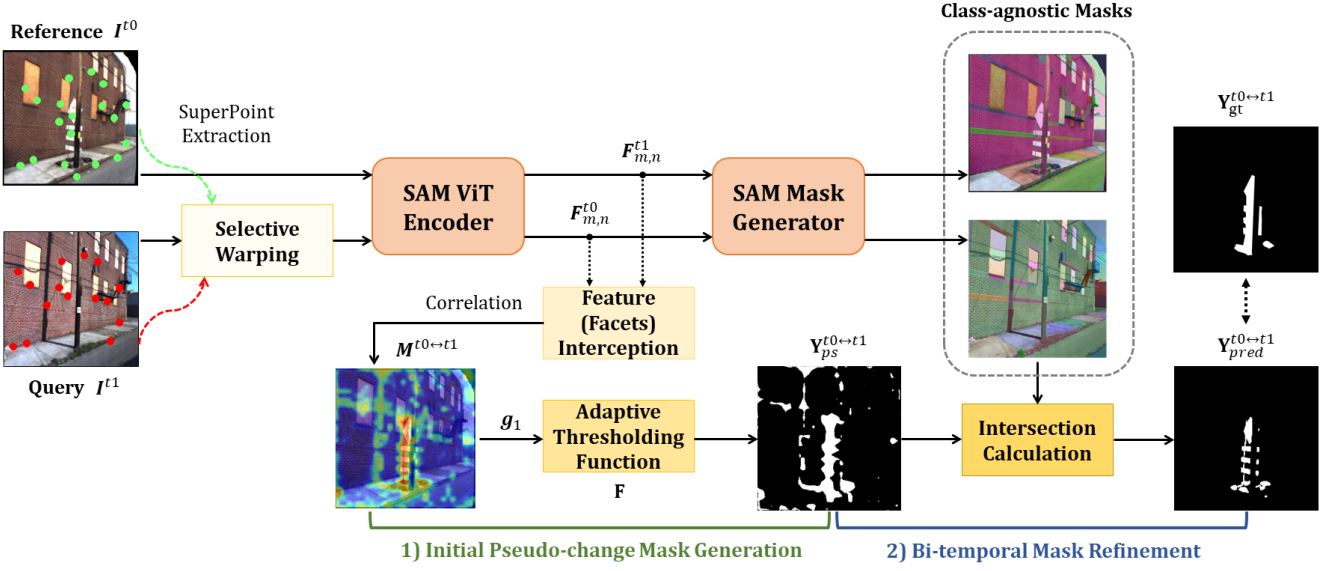


Figure 1: Illustration of the proposed GeSCF pipeline. We intercept the facet features from SAM ViT and correlate them to get a similarity distribution. Further, we utilize the SAM mask generator to refine initial pseudo-change masks. GeSCF consists of two major steps: 1) initial pseudo-change mask generation and 2) bi-temporal mask refinement.

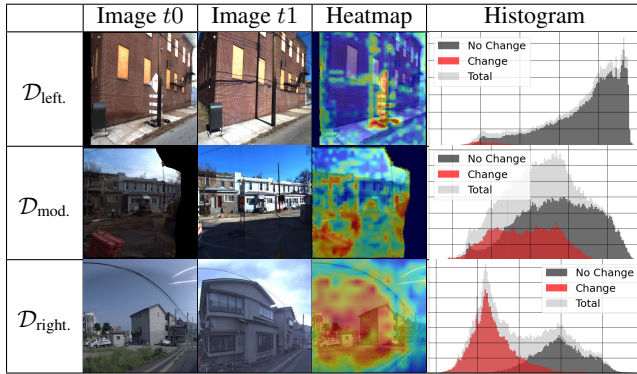


Figure 2: Examples of left-skewed ( $\mathcal{D}_{\text{left.}}$ ), moderate ( $\mathcal{D}_{\text{mod.}}$ ), and right-skewed ( $\mathcal{D}_{\text{right.}}$ ) similarity distribution obtained through the foundation model. We visualize the heatmaps and histograms. We plot histograms for each pixel in the distribution as Change, No Change, and Total, respectively.

## Generalizable Scene Change Detection Framework

### Motivation and Overview

We aim to incorporate robust features from a foundation model to make a generalizable SCD algorithm over temporal conditions and unseen domains. The key idea of GeSCF is as follows: we intercept and correlate the foundation model’s features to get rich *similarity distribution* and transform them into binary pseudo-change masks by adaptively thresholding the low-similarity pixels with a skewness-based algorithm, unlike previous approaches that directly transfer the features from the pre-trained model. Moreover, We uti-

lize a warping module that selectively estimates the homography and warps the image to improve the correlation accuracy—handling imperfect matches as well. Finally, we refine pseudo-change masks leveraging SAM to generate fine-grained change masks. Overall, GeSCF includes two stages: initial pseudo-change mask generation and bi-temporal mask refinement (see Fig. 1).

### Similarity Distribution and Sample Skewness

Inspired by previous studies (Amir et al. 2021; Caron et al. 2021; Kirillov et al. 2023) that have empirically demonstrated that attention maps can capture semantically salient objects, we correlate facet features (one of Key, Query, and Value) from the SAM ViT layer. Specifically, given a bi-temporal RGB image pair ( $I^{t0}, I^{t1}$ ), we intercept the facet embeddings  $\mathbf{F}^{t0}_{m,n}, \mathbf{F}^{t1}_{m,n} \in \mathbb{R}^{N \times H \times W}$  respectively, for the  $m$ -th head from the  $n$ -th ViT layer. Then, we compute similarity distribution  $\mathbf{M}^{t0 \leftrightarrow t1}$  of image pair as follows:

$$\mathbf{P}^{t0 \leftrightarrow t1}_{m,n} = \mathbf{F}^{t0}_{m,n}^\top \mathbf{F}^{t1}_{m,n}, \quad (1)$$

$$\mathbf{M}^{t0 \leftrightarrow t1} = \xi \left( \sum_{m=1}^M \mathbf{P}^{t0 \leftrightarrow t1}_{m,n} \right) \quad (2)$$

where  $\xi(\cdot)$  performs spatial reshaping and bilinear interpolation to the input image size. The correlation in (1) is a commutative operation that generates identical distribution even with the reversed order. Furthermore, we compute the sample skewness  $g_1$  of the distribution as follows:

$$g_1 = \frac{k}{(k-1)(k-2)} \sum_i^k \left( \frac{m_i - \bar{m}}{s} \right)^3, \quad (3)$$

where  $m_i$  are the pixel similarity,  $\bar{m}$  is the mean value,  $s$  is the standard deviation, and  $k$  is the number of pixels in the distribution.

As illustrated in Fig. 2, the feature similarity distribution of SAM can capture semantically meaningful changes in the scene. Moreover, the distribution falls into three categories depending on the sample skewness. The specific definitions for partitioning image pairs are as follows:

$$\begin{aligned}\mathcal{D}_{\text{left-skewed}} &= \{\mathcal{I} = (I^{t0}, I^{t1}) \mid g_1 \leq \mathbf{N}_i\}, \\ \mathcal{D}_{\text{moderate}} &= \{\mathcal{I} = (I^{t0}, I^{t1}) \mid \mathbf{N}_i < g_1 < \mathbf{N}_j\}, \\ \mathcal{D}_{\text{right-skewed}} &= \{\mathcal{I} = (I^{t0}, I^{t1}) \mid g_1 \geq \mathbf{N}_j\},\end{aligned}$$

where  $N_i$  and  $N_j$  are constant hyperparameters. To precisely pinpoint changes, it is essential to consider skewness, reflecting the context of the scene changes. For example, if a significant change has occurred, such as the construction or de-construction of a building, we should consider large bulks on the left side of the distribution as changes.

### Initial Pseudo-change Mask Generation

**Initial Pseudo-change Mask:** With the similarity distribution  $\mathbf{M}^{t0 \leftrightarrow t1}$  and sample skewness  $g_1$ , we generate initial pseudo-change mask  $\mathbf{Y}_{ps}^{t0 \leftrightarrow t1}$  as follows:

$$\mathbf{Y}_{ps}^{t0 \leftrightarrow t1} = \begin{cases} \mathbf{\Pi}(\hat{\mathcal{Z}}(\mathbf{M}^{t0 \leftrightarrow t1}), \mathbf{F}(g_1)), & \mathcal{I} \in \mathcal{D}_{\text{skewed}} \\ \mathbf{\Pi}(\mathcal{Z}(\mathbf{M}^{t0 \leftrightarrow t1}), \mathbf{F}(g_1)), & \mathcal{I} \in \mathcal{D}_{\text{moderate}} \end{cases} \quad (4)$$

where  $\mathcal{Z}$  and  $\hat{\mathcal{Z}}$  refer to Z-score and modified Z-score, respectively,  $\mathbf{F}(\cdot)$  is an adaptive thresholding function and  $\mathbf{\Pi}(\cdot)$  applies an element-wise binary threshold computed from  $\mathbf{F}(\cdot)$  that formulates similarity distribution into binary change masks. Modified Z-score, or Median Absolute Deviation (MAD), is a simple and effective statistical method to detect outliers in the skewed distribution.

**Adaptive Thresholding Function:** Instead of using several constant thresholds for different change types, we define an adaptive thresholding function to elaborate the threshold from two perspectives. One is the different base thresholds in each case; we apply a much lower threshold for right-skewed cases than left-skewed cases to reflect the context of the changes mentioned above. The other is the awareness of the long-tail and bulk distribution; we avoid encountering sharp drops or rises in the distributions by strengthening the threshold to the highly skewed cases. Finally, we define the thresholding function as:

$$\mathbf{F}(g_1) = \begin{cases} \mathbf{B}_{\text{left}} - \mathbf{c}_k \cdot \mathbf{S}_{\text{left}} \cdot g_1, & \mathcal{I} \in \mathcal{D}_{\text{left-skewed}} \\ \mathbf{Z}_c, & \mathcal{I} \in \mathcal{D}_{\text{moderate}} \\ \mathbf{B}_{\text{right}} + \mathbf{c}_k \cdot \mathbf{S}_{\text{right}} \cdot g_1, & \mathcal{I} \in \mathcal{D}_{\text{right-skewed}} \end{cases}, \quad (5)$$

where  $\mathbf{B}_{\text{left}}$  and  $\mathbf{B}_{\text{right}}$  refer to the base thresholds,  $\mathbf{S}_{\text{left}}$  and  $\mathbf{S}_{\text{right}}$  represent the sensitivity to the each skewness.  $\mathbf{c}_k$  is a normalization factor regarding  $k$  and  $\mathbf{Z}_c$  corresponds to  $z$

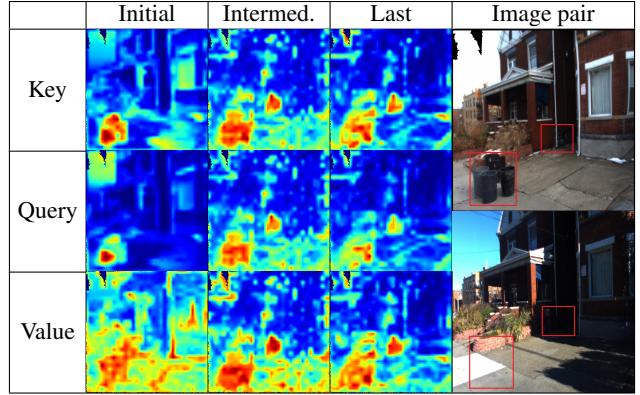


Figure 3: Visualization of the similarity distribution depending on the facets and the layers. The changed regions of the image pair are indicated with a red bounding box.

value with confidence  $c$ . This function adjusts the criteria for converting similarity distribution into a binary change mask.

**Selective Warping:** To handle imperfect matches between image pairs, we adopt coarse alignment using homography estimation to acquire enhanced similarity distribution. We employ SuperPoint (DeTone, Malisiewicz, and Rabenovich 2017) to extract local keypoints from each temporal image and estimate homography matrix  $\mathbf{H}$ . We selectively warp images that display a sufficient inlier ratio of matched keypoints. This strategy ensures the stability of warped images by filtering out the image pair for which matching keypoints is difficult due to significant changes—resulting in a more reliable initial pseudo-change mask.

**Choice of Layer and Facet:** Selecting a particular layer and facet from a pre-trained SAM ViT constitutes a crucial design aspect of the GeSCF. We focus on two pivotal factors: homogeneity and contrast. As shown in Fig. 3, the Key and Query in the intermediate layer demonstrate a notable homogeneity within areas of change and a clear contrast with the surrounding unchanged areas, compared to the Value facet. Moreover, they capture changes affected by low illumination, a challenge not adequately addressed in the initial layer. The last layer lacks homogeneity in the changed areas, highlighting part or subpart of the changes. Therefore, we intercept Key features from the intermediate layer that exhibit lower similarity scores in the changed region. For more examples and analysis, please refer to the supplementary material.

### Bi-temporal Mask Refinement

Although similarity distribution and homography warping provide reasonable pseudo masks for the possible changes, a set of unchanged parts of the distribution hold low similarity scores and depth variation during transformation creates noise in the initial pseudo-change masks. To resolve this, we leverage SAM masks to obtain detailed location and structure of the scene semantics. We calculate the intersection between pseudo-change masks and SAM-generated class-agnostic masks to obtain high-quality change masks. We select masks that show  $\alpha > \alpha_t$  as the final mask  $\mathbf{Y}_{pred}^{t0 \leftrightarrow t1}$ , where

Dataset	Environment					#.	Type
	U	S	R	I	D		
VL-CMU-CD	✓					429	Real
TSUNAMI	✓				✓	100	Real
ChangeSim				✓		8,212	Sim.
<b>ChangeVPR</b>	✓	✓	✓			529	Real

Table 2: Summary of the datasets for evaluation. Each symbol represents Urban (U), Suburban (S), Rural (R), Indoor (I), and Disaster (D), respectively.

$\alpha$  refers to the percentage of overlap and  $\alpha_t$  is a corresponding threshold. Since changes can occur bi-temporally, we apply the refinement for both  $t0$  and  $t1$  images—maintaining commutativity for the proposed GeSCF.

### Generalizable Scene Change Detection

**Overview:** We propose GeSCD with novel metrics, evaluation dataset, and evaluation protocol to address the generalizability over unseen domains and robustness under different temporal conditions of SCD algorithms. Our task approach, distinctive from conventional methods, effectively addresses the critical need for SCD research that is genuinely generalizable and effective across diverse settings.

**Metrics:** We report the F1-score, the harmonic mean of precision and recall, for both temporal directions, in contrast to previous methods that only report the performance of a single temporal prediction. Furthermore, we propose Temporal Consistency (TC) by measuring the union intersection between  $t0 \rightarrow t1$  ( $t0$ ) and  $t1 \rightarrow t0$  ( $t1$ ) predictions as follows:

$$\text{Temporal Consistency (TC)} = \frac{\mathbf{Y}_{pred}^{t0 \rightarrow t1} \cap \mathbf{Y}_{pred}^{t1 \rightarrow t0}}{\mathbf{Y}_{pred}^{t0 \rightarrow t1} \cup \mathbf{Y}_{pred}^{t1 \rightarrow t0}}, \quad (6)$$

where the proposed TC score indicates how much the SCD algorithms can generate consistent change masks in bi-directional orders.

**Evaluation Datasets:** Table 2 summarizes the evaluation datasets. First, we consider three standard SCD datasets with different characteristics: VL-CMU-CD (Alcantarilla et al. 2016), TSUNAMI (Sakurada and Okatani 2015), and ChangeSim (Park et al. 2021). These datasets represent urban environments in the USA, disaster-impacted urban areas in Japan, and industrial indoor settings within simulation environments, respectively. Furthermore, for the quantitative evaluation of the proposed generalizable approach, we create a new dataset named the **ChangeVPR**. The ChangeVPR comprises 529 image pairs collected from the SF-XL (Bertoni, Masone, and Caputo 2022), St Lucia (Milford and Wyeth 2008), and Nordland (Sünderhauf, Neubert, and Protzel 2013) datasets, which are widely used in Visual Place Recognition (VPR) research. We carefully sampled image pairs from each dataset to reflect various SCD challenges such as weather conditions and seasonal changes, and hand-labeled the ground-truth change masks for image

pairs<sup>1</sup>. We use the ChangeVPR only for the evaluation to assess unseen domain performance. For more details about the dataset, please refer to the supplementary material.

**Evaluation Protocol:** We train each model on the three standard SCD datasets; the training stage results in three distinctive models for each method. Then, we assess each of the three distinctive models in two stages. First, we evaluate the three models on the three conventional SCD datasets; this process totals nine assessments. If the method of interest does not involve training, we evaluate the model on the three datasets (three assessments). Next, we evaluate the models on the proposed ChangeVPR. Since we use the ChangeVPR only for the evaluation, this stage contains three assessments per model (due to three splits of ChangeVPR). As a result, the proposed protocol estimates performance on both seen and unseen domain datasets.

## Results and Analysis

### Implementation Details

We use the SAM ViT-H encoder, pre-trained on the SA-1B dataset, to extract facet features and obtain initial pseudo-change masks. We set  $N_i = -0.2$ ,  $N_j = 0.2$ , and  $c = -0.52$  to categorize the distribution types. For adaptive thresholding function, we set  $B_{left} = 0.7$ ,  $B_{right} = 0.1$ ,  $S_{left} = 1.0$ , and  $S_{right} = 0.1$ . Especially, GeSCF requires no further tuning for handling unseen data—sharing the same hyperparameters.

### Comparative Studies

We compare our method with four open-source deep learning-based SCD algorithms: CSCDNet, CDResNet (Sakurada, Shibuya, and Wang 2018), DR-TANet, and C-3PO. For the C-3PO, we adopt the (I+D) structure for the VL-CMU-CD and the (I+A+D+E) structure for the TSUNAMI and ChangeSim datasets, following the configurations proposed in the paper. For the ChangeVPR, we display baselines trained on the VL-CMU-CD, which contains more general images than the others. Further comparisons are provided in the supplementary material.

**Quantitative Comparison:** Table 3 displays the quantitative comparison results on the standard SCD datasets. The results attest that GeSCF outperforms the baselines with a large margin in every unseen domain (off-diagonal results) and on-par performance on seen domains (diagonal results), along with perfect temporal consistency for all settings. The symmetry of C-3PO does not hold for the VL-CMU-CD, as expected by the low TC score of 0.02. Moreover, GeSCF outperforms the baselines with in-domain settings for the ChangeSim. Overall, the average performance of our method is 65.0%, surpassing the second-best of 48.5% trained on the TSUNAMI by a substantial margin. Table 4 presents the quantitative comparison results on the proposed ChangeVPR. The results consistently demonstrate that GeSCF outperforms the baseline on every unseen domains, extending beyond the conventional SCD domains.

<sup>1</sup>The SCD task generally requires VPR systems to pair the current scene with scenes stored in a database (Park et al. 2022). However, existing real-world SCD datasets, which only contain a few urban scenarios, do not reflect the diversity of the VPR systems.

Method	Training	VL-CMU-CD			TSUNAMI			ChangeSim			Avg.
		<i>t</i> 0	<i>t</i> 1	TC	<i>t</i> 0	<i>t</i> 1	TC	<i>t</i> 0	<i>t</i> 1	TC	
CSCDNet	VL-CMU-CD	77.4	4.5	0.02	5.6	19.4	0.02	25.5	13.6	0.09	24.3
CDResNet		74.7	2.1	0.01	2.3	4.6	0.0	25.4	13.2	0.12	20.4
DR-TANet		74.2	1.6	0.01	2.6	6.7	0.0	27.5	18.0	0.19	21.8
C-3PO		<b>77.6</b>	4.6	0.02	8.0	34.3	0.02	30.4	21.0	0.16	29.3
CSCDNet	TSUNAMI	17.0	22.1	0.4	83.6	60.3	0.46	27.8	30.5	0.29	40.2
CDResNet		13.2	18.4	0.42	82.8	51.5	0.38	26.3	29.0	0.31	36.9
DR-TANet		14.8	17.3	0.53	82.0	57.6	0.44	24.4	26.8	0.35	37.2
C-3PO		27.0	27.0	1.0	<b>84.2</b>	<b>84.2</b>	1.0	34.3	34.3	1.0	48.5
CSCDNet	ChangeSim	20.1	3.5	0.04	2.5	6.6	0.01	43.1	18.9	0.31	15.8
CDResNet		17.5	3.1	0.02	4.6	9.9	0.01	41.3	18.2	0.18	15.8
DR-TANet		20.3	4.9	0.05	5.0	8.3	0.01	40.3	18.0	0.18	16.1
C-3PO		1.6	1.6	1.0	0.3	0.3	1.0	15.8	15.8	1.0	5.9
GeSCF (Ours)	Zero-shot	71.2	<b>71.2</b>	<b>1.0</b>	70.1	70.1	<b>1.0</b>	<b>53.8</b>	<b>53.8</b>	<b>1.0</b>	<b>65.0</b>

Table 3: Quantitative results of methods on standard SCD datasets.

Method	SF-XL (U)			St Lucia (S)			Nordland (R)			Avg.
	<i>t</i> 0	<i>t</i> 1	TC	<i>t</i> 0	<i>t</i> 1	TC	<i>t</i> 0	<i>t</i> 1	TC	
CSCDNet	28.6	23.1	0.07	11.8	15.3	0.27	14.3	5.8	0.33	16.5
CDResNet	22.9	18.9	0.08	13.5	18.0	0.18	9.3	6.7	0.39	14.9
DR-TANet	22.5	19.6	0.05	15.5	20.8	0.19	11.9	8.2	0.33	16.4
C-3PO	38.7	32.8	0.07	21.7	25.7	0.14	16.2	14.2	0.28	24.9
GeSCF (Ours)	<b>66.9</b>	<b>66.9</b>	<b>1.0</b>	<b>54.6</b>	<b>54.6</b>	<b>1.0</b>	<b>53.2</b>	<b>53.2</b>	<b>1.0</b>	<b>58.2</b>

Table 4: Quantitative results of methods on ChangeVPR. We present baselines trained on the VL-CMU-CD.

Method	VL-CMU-CD		TSUNAMI		Change Sim		Avg.
	<i>t</i> 0, 1	TC	<i>t</i> 0, 1	TC	<i>t</i> 0, 1	TC	
CSCDNet	64.5	0.61	8.0	0.12	23.9	0.42	32.1
CDResNet	61.2	0.58	4.4	0.18	15.9	0.29	27.2
DR-TANet	53.7	0.40	2.4	0.02	20.5	0.26	25.5
C-3PO	61.0	0.63	2.0	0.07	22.5	0.51	28.5
GeSCF (Ours)	<b>71.2</b>	<b>1.0</b>	<b>70.1</b>	<b>1.0</b>	<b>53.8</b>	<b>1.0</b>	<b>65.0</b>

Table 5: Quantitative results of methods bi-temporally trained on VL-CMU-CD. We use the average F1-score (*t*0, 1) between two temporal predictions.

Component	Method	VL-CMU-CD	TSUNAMI	Change Sim
Adaptive Thresholding Function	Z-score	54.9	69.2	43.0
	MAD	58.5	70.0	45.3
	<b>Ours</b>	<b>71.2</b>	<b>70.1</b>	<b>53.8</b>
Selective Warping	No warp	70.7	64.4	36.4
	All warp	68.0	55.3	51.9
Mask Refinement	<b>Ours</b>	<b>71.2</b>	<b>70.1</b>	<b>53.8</b>
	Pseudo.	53.3	60.0	47.3
<b>+Refine.</b>	<b>71.2</b>	<b>70.1</b>	<b>53.8</b>	

Table 6: Ablations and comparisons.

**Analysis on Bi-temporal Training:** In Table 5, we present quantitative results of each baseline trained with bi-temporal objective (Zheng et al. 2021). The results demonstrate that simple bi-temporal training does not guarantee complete temporal consistency and unseen domain performance—even worsening the uni-temporal performances in Table 3.

**Qualitative Comparison:** The ChangeVPR dataset involves various challenging scenarios tailored for GeSCD, including background/foreground changes, illumination variations, weather conditions, seasonal changes, and day/night transitions (see Fig. 4). The qualitative results corroborate

that GeSCF robustly captures changed semantics of unseen domains under challenging conditions, while other methods fail. Moreover, as a zero-shot framework, GeSCF does not learn annotation biases in a dataset (see Fig. 5). For instance, GeSCF generates a more accurate mask for the artifact and identifies un-annotated changes, such as a sign, a basket, and a car. These results suggest that GeSCF’s outputs are more reasonable than baselines, even though its quantitative results are lower for some samples in in-domain settings.

	Image $t0$	Image $t1$	CSCDNet	CDResNet	DR-TANet	C-3PO	Ours	GT
Background/ Foreground Changes								
Illumination Variations								
Weather Conditions								
Seasonal Changes								
Seasonal, Day/night Transitions								

Figure 4: Qualitative results of methods on ChangeVPR. We present baselines trained on the VL-CMU-CD.

Image $t0$	Image $t1$	CSCDNet	CDResNet	DR-TANet	C-3PO	Ours	GT
		<i>F1: 84.5</i>	<i>F1: 79.9</i>	<i>F1: 68.9</i>	<i>F1: 71.4</i>	<i>F1: 66.3</i>	
		<i>F1: 24.6</i>	<i>F1: 20.5</i>	<i>F1: 17.0</i>	<i>F1: 32.5</i>	<i>F1: 15.2</i>	

Figure 5: Qualitative results of methods on VL-CMU-CD with F1-scores. We present baselines of in-domain settings.

## Ablation Studies

We conduct a component-wise analysis of GeSCF. Table 6 shows the quantitative results of the ablations.

**Effect of Adaptive Thresholding Function:** We implement thresholding functions with various statistical methods that utilize constant thresholds, including Z-score and Modified Z-score. Experiments show that Modified Z-score obtains better performance than the naive Z-score, while our skewness-based adaptive method achieves the best.

**Effect of Selective Warping:** In the VL-CMU-CD and TSUNAMI datasets which mostly contains image pairs with almost perfect alignment, warping all the images obtains lower performance than not warping. On the contrary, ChangeSim shows the significant performance gain through warping, where the dataset contains a lot of imperfectly matched image pairs. Overall, our selective warping yields the best performance in all settings.

**Effect of Mask Refinement:** We report the performance of the model solely using initial pseudo-change masks. Al-

though the overall performance is lower than that of the final model, it effectively contains the changed region, which could be further improved through mask refinement.

## Conclusion

In this study, we attempted to address the generalization of SCD using a foundation model for the first time to the best of our knowledge; we define GeSCD along with the novel metrics, evaluation dataset (ChangeVPR), and evaluation protocols to effectively assess the generalizability of SCD models. Further, we proposed GeSCF, a generalizable approach for the SCD task using the localized semantics of the foundation model that does not require costly SCD labeling. Extensive experiments demonstrated that the proposed GeSCF significantly outperforms existing SCD models on unseen domains and matches fine-tuned models on seen domains while achieving complete temporal consistency. We expect our methods can serve as a solid step towards robust and generalizable Scene Change Detection research.

## References

Ahmadi, M.; Lonbar, A. G.; Sharifi, A.; Beris, A. T.; Nouri, M. J.; and Javidi, A. S. 2023. Application of Segment Anything Model for Civil Infrastructure Defect Assessment. *ArXiv*, abs/2304.12600.

Akilan, T.; Wu, Q.; Safaei, A.; Huo, J.; and Yang, Y. 2020. A 3D CNN-LSTM-Based Image-to-Image Foreground Segmentation. *IEEE Transactions on Intelligent Transportation Systems*, 21: 959–971.

Alcantarilla, P. F.; Stent, S.; Ros, G.; Arroyo, R.; and Gherardi, R. 2016. Street-view change detection with deconvolutional networks. *Autonomous Robots*, 42: 1301 – 1322.

Amir, S.; Gandsman, Y.; Bagon, S.; and Dekel, T. 2021. Deep ViT Features as Dense Visual Descriptors. *ArXiv*, abs/2112.05814.

Bandara, W. G. C.; and Patel, V. M. 2022. Revisiting Consistency Regularization for Semi-supervised Change Detection in Remote Sensing Images. *ArXiv*, abs/2204.08454.

Bergamasco, L.; Saha, S.; Bovolo, F.; and Bruzzone, L. 2022. Unsupervised Change Detection Using Convolutional-Autoencoder Multiresolution Features. *IEEE Transactions on Geoscience and Remote Sensing*, 60: 1–19.

Bernhard, M.; Strauß, N.; and Schubert, M. 2023. MapFormer: Boosting Change Detection by Using Pre-change Information. *2023 IEEE/CVF International Conference on Computer Vision (ICCV)*, 16791–16800.

Bertoni, G.; Masone, C. G.; and Caputo, B. 2022. Rethinking Visual Geo-localization for Large-Scale Applications. *2022 IEEE/CVF Conference on Computer Vision and Pattern Recognition (CVPR)*, 4868–4878.

Caron, M.; Touvron, H.; Misra, I.; J'egou, H.; Mairal, J.; Bojanowski, P.; and Joulin, A. 2021. Emerging Properties in Self-Supervised Vision Transformers. *2021 IEEE/CVF International Conference on Computer Vision (ICCV)*, 9630–9640.

Chen, C.; Hsieh, J.-W.; Chen, P.-Y.; Hsieh, Y.-K.; and Wang, B. 2022. SARAS-Net: Scale and Relation Aware Siamese Network for Change Detection. *ArXiv*, abs/2212.01287.

Chen, S.; Yang, K.; and Stiefelhagen, R. 2021. DR-TANet: Dynamic Receptive Temporal Attention Network for Street Scene Change Detection. *2021 IEEE Intelligent Vehicles Symposium (IV)*, 502–509.

Chen, T.; Mai, Z.; Li, R.; and Chao, W.-L. 2023. Segment Anything Model (SAM) Enhanced Pseudo Labels for Weakly Supervised Semantic Segmentation. *ArXiv*, abs/2305.05803.

Chen, Y.; and Bruzzone, L. 2022. A Self-Supervised Approach to Pixel-Level Change Detection in Bi-Temporal RS Images. *IEEE Transactions on Geoscience and Remote Sensing*, 60: 1–11.

DeTone, D.; Malisiewicz, T.; and Rabinovich, A. 2017. SuperPoint: Self-Supervised Interest Point Detection and Description. *2018 IEEE/CVF Conference on Computer Vision and Pattern Recognition Workshops (CVPRW)*, 337–33712.

Ding, L.; Zhu, K.; Peng, D.; Tang, H.; Yang, K.; and Bruzzone, L. 2023. Adapting Segment Anything Model for Change Detection in VHR Remote Sensing Images. *IEEE Transactions on Geoscience and Remote Sensing*, 62: 1–11.

Dosovitskiy, A.; Beyer, L.; Kolesnikov, A.; Weissenborn, D.; Zhai, X.; Unterthiner, T.; Dehghani, M.; Minderer, M.; Heigold, G.; Gelly, S.; Uszkoreit, J.; and Houlsby, N. 2020. An Image is Worth 16x16 Words: Transformers for Image Recognition at Scale. *ArXiv*, abs/2010.11929.

Dosovitskiy, A.; Fischer, P.; Ilg, E.; Häusser, P.; Hazirbas, C.; Golkov, V.; van der Smagt, P.; Cremers, D.; and Brox, T. 2015. FlowNet: Learning Optical Flow with Convolutional Networks. *2015 IEEE International Conference on Computer Vision (ICCV)*, 2758–2766.

Giannakis, I.; Bhardwaj, A.; Sam, L.; and Leontidis, G. 2023. Deep learning universal crater detection using Segment Anything Model (SAM). *ArXiv*, abs/2304.07764.

Hao, F.; Ma, Z.; peng Tian, H.; Wang, H.; and Wu, D. 2023. Semi-supervised label propagation for multi-source remote sensing image change detection. *Comput. Geosci.*, 170: 105249.

Huang, C.; Guan, H.; Jiang, A.; Zhang, Y.; Spratling, M. W.; and Wang, Y. 2022. Registration based Few-Shot Anomaly Detection. In *European Conference on Computer Vision (ECCV)*.

Janai, J.; Güney, F.; Behl, A.; and Geiger, A. 2017. Computer Vision for Autonomous Vehicles: Problems, Datasets and State-of-the-Art. *Found. Trends Comput. Graph. Vis.*, 12: 1–308.

Kirillov, A.; Mintun, E.; Ravi, N.; Mao, H.; Rolland, C.; Gustafson, L.; Xiao, T.; Whitehead, S.; Berg, A. C.; Lo, W.-Y.; Dollár, P.; and Girshick, R. B. 2023. Segment Anything. *2023 IEEE/CVF International Conference on Computer Vision (ICCV)*, 3992–4003.

Lee, S.; and Kim, J.-H. 2024. Semi-Supervised Scene Change Detection by Distillation from Feature-metric Alignment. *2024 IEEE/CVF Winter Conference on Applications of Computer Vision (WACV)*, 1215–1224.

Mandal, M.; Dhar, V.; Mishra, A.; Vipparthi, S. K.; and Abdel-Mottaleb, M. 2020. 3DCD: Scene Independent End-to-End Spatiotemporal Feature Learning Framework for Change Detection in Unseen Videos. *IEEE Transactions on Image Processing*, 30: 546–558.

Mei, L.; Ye, Z.; Xu, C.; Wang, H.; Wang, Y.; Lei, C.; Yang, W.; and Li, Y. 2024. SCD-SAM: Adapting Segment Anything Model for Semantic Change Detection in Remote Sensing Imagery. *IEEE Transactions on Geoscience and Remote Sensing*, 62: 1–13.

Milford, M.; and Wyeth, G. F. 2008. Mapping a Suburb With a Single Camera Using a Biologically Inspired SLAM System. *IEEE Transactions on Robotics*, 24: 1038–1053.

Mu, N.; Kirillov, A.; Wagner, D.; and Xie, S. 2022. Slip: Self-supervision meets language-image pre-training. In *European Conference on Computer Vision (ECCV)*, 529–544. Springer.

Nehmzow, U.; Kuljis, J.; Paul, R. J.; and Thomas, P. 2000. Mobile Robotics: A Practical Introduction: History, Design, Analysis and Examples.

Noh, H.; Ju, J.; seek Seo, M.; chan Park, J.; and geol Choi, D. 2022. Unsupervised Change Detection Based on Image Reconstruction Loss. *2022 IEEE/CVF Conference on Computer Vision and Pattern Recognition Workshops (CVPRW)*, 1351–1360.

Oquab, M.; Dariset, T.; Moutakanni, T.; Vo, H. Q.; Szafraniec, M.; Khalidov, V.; Fernandez, P.; Haziza, D.; Massa, F.; El-Nouby, A.; Assran, M.; Ballas, N.; Galuba, W.; Howes, R.; Huang, P.-Y. B.; Li, S.-W.; Misra, I.; Rabat, M. G.; Sharma, V.; Synnaeve, G.; Xu, H.; Jégou, H.; Mairal, J.; Labatut, P.; Joulin, A.; and Bojanowski, P. 2023. DINOv2: Learning Robust Visual Features without Supervision. *ArXiv*, abs/2304.07193.

Park, J.-M.; Jang, J.-H.; Yoo, S.-M.; Lee, S.-K.; Kim, U.-H.; and Kim, J.-H. 2021. ChangeSim: Towards End-to-End Online Scene Change Detection in Industrial Indoor Environments. *2021 IEEE/RSJ International Conference on Intelligent Robots and Systems (IROS)*, 8578–8585.

Park, J.-M.; Kim, U.-H.; Lee, S.; and Kim, J.-H. 2022. Dual Task Learning by Leveraging Both Dense Correspondence and Mis-Correspondence for Robust Change Detection With Imperfect Matches. *2022 IEEE/CVF Conference on Computer Vision and Pattern Recognition (CVPR)*, 13739–13749.

Radford, A.; Kim, J. W.; Hallacy, C.; Ramesh, A.; Goh, G.; Agarwal, S.; Sastry, G.; Askell, A.; Mishkin, P.; Clark, J.; Krueger, G.; and Sutskever, I. 2021. Learning Transferable Visual Models From Natural Language Supervision. In *International Conference on Machine Learning (ICML)*.

Radke, R. J.; Andra, S.; Al-Kofahi, O.; and Roysam, B. 2005. Image change detection algorithms: a systematic survey. *IEEE Transactions on Image Processing*, 14: 294–307.

Ramkumar, V. R. T.; Arani, E.; and Zonooz, B. 2022. Differencing based Self-supervised pretraining for Scene Change Detection. In *CoLLAs*.

Saha, S.; Shahzad, M.; Ebel, P.; and Zhu, X. X. 2022. Supervised Change Detection Using Prechange Optical-SAR and Postchange SAR Data. *IEEE Journal of Selected Topics in Applied Earth Observations and Remote Sensing*, 15: 8170–8178.

Sakurada, K.; and Okatani, T. 2015. Change Detection from a Street Image Pair using CNN Features and Superpixel Segmentation. In *British Machine Vision Conference (BMVC)*.

Sakurada, K.; Shibuya, M.; and Wang, W. 2018. Weakly Supervised Silhouette-based Semantic Scene Change Detection. *2020 IEEE International Conference on Robotics and Automation (ICRA)*, 6861–6867.

Sakurada, K.; Wang, W.; Kawaguchi, N.; and Nakamura, R. 2017. Dense Optical Flow based Change Detection Network Robust to Difference of Camera Viewpoints. *ArXiv*, abs/1712.02941.

Sünderhauf, N.; Neubert, P.; and Protzel, P. 2013. Are We There Yet? Challenging SeqSLAM on a 3000 km Journey Across All Four Seasons.

Wang, G.-H.; Gao, B.-B.; and Wang, C. 2023. How to Reduce Change Detection to Semantic Segmentation. *Pattern Recognition*, 138: 109384.

Wu, G.; Zheng, Y.; Guo, Z.; Cai, Z.; Shi, X.; Ding, X.; Huang, Y.; Guo, Y.; and Shibasaki, R. 2020. Learn to recover visible color for video surveillance in a day. In *European Conference on Computer Vision (ECCV)*, 495–511. Springer.

Xie, D.; Wang, R.; Ma, J.; Chen, C.; Lu, H.; Yang, D.; Shi, F.; and Lin, X. 2023. Edit Everything: A Text-Guided Generative System for Images Editing. *ArXiv*, abs/2304.14006.

Yu, T.; Feng, R.; Feng, R.; Liu, J.; Jin, X.; Zeng, W.; and Chen, Z. 2023. Inpaint Anything: Segment Anything Meets Image Inpainting. *ArXiv*, abs/2304.06790.

Zheng, Z.; Ma, A.; Zhang, L.; and Zhong, Y. 2021. Change is Everywhere: Single-Temporal Supervised Object Change Detection in Remote Sensing Imagery. *2021 IEEE/CVF International Conference on Computer Vision (ICCV)*, 15173–15182.